Photon Mapping of Geometrically Complex Glass Structures: Methods and Experimental Evaluation

Ramon E. Weber*[a], Christoph Reinhart[b], and Neri Oxman[a]

[a] Mediated Matter Group, MIT Media Lab, Department of Architecture and Urban Planning,
Massachusetts Institute of Technology, 75 Amherst St, Cambridge, MA 02139, USA
T +1 617 324 3626
*reweber@mit.edu [corresponding author], neri@mit.edu

[b] Sustainable Design Lab, Department of Architecture and Urban Planning,
Massachusetts Institute of Technology, 77 Massachusetts Avenue, Cambridge, MA 02139, USA
T +1 617-253-7714
tito_@mit.edu

Abstract

Advances in digital fabrication and additive manufacturing have enabled the creation of geometrically complex glass structures and building components, opening up new design opportunities across scales. Quantifying and evaluating their optical performance, however, remains a technical challenge. In order to accurately predict light behavior, common approaches of daylight modelling utilizing light-backward raytracers are insufficient. This paper evaluates the use of the photon mapping approach within the *Radiance* render engine to simulate artificial and natural lighting conditions. 3D printed optically transparent glass components are used to benchmark the simulations. We present a workflow to gather geometric data of the glass objects and a series of validation experiments. Pairs of physical studies and digital simulations are compared to assess optical performance in the context of both indoor and outdoor lighting conditions. These experiments demonstrate that the photon mapping approach can reliably measure and predict caustic light patterns and indoor light levels with some limitations, specifically of glare and scattered light from the glass objects themselves.

(163 words)

Keywords: photon map, raytracing, daylight simulation, 3D printing, glass

1 Introduction

Lighting the built environment is one of the foundations of modern life with direct consequences for our everyday experiences, the environment, and workplace productivity. The way we choose to light the interior of our buildings, using a combination of daylight and electric lighting, quite literally determines how and what we see. However, electric lighting comes at a significant cost, accounting for 17% of U.S. energy use in commercial buildings [1]. Daylighting has been widely promoted, not merely as an electric lighting replacement, but as a superior source of lighting due to its spectral qualities, ability to offer views, and temporal variability that links building occupants to the outside. While increasingly dense urban environments challenge access to daylight for all, thoughtful urban zoning and building massing approaches can support good daylight penetration even in unusually dense urban environments [2]. In order to explore lighting and daylighting concepts in non-standard situations, architectural design teams routinely rely on an ever-expanding suite of simulation tools for both electric lighting as well as daylighting design [3]. While a variety of simulation approaches exist for modeling daylight, the open source light-backward raytracer, *Radiance* [4], written by Greg Ward at Lawrence Berkley National Laboratory, has dominated the field of sustainable building design for decades [5]. Part of the appeal of *Radiance* is that it has been extensively validated vis-à-vis measurements in full–scale mockups both for illuminance distributions [6–9] and high dynamic range (HDR) luminance distributions [10]. Furthermore, non-expert user-friendly implementations of *Radiance* in popular

software tools such as DIVA [11] and Ladybug Tools [12] are becoming popular amongst architects and engineers and enable predictions of daylight availability or glare during the building design process.

However, as with any light-backward raytracer, *Radiance* cannot reliably model light-concentrating phenomena such as caustics from lenses or curved highly special surfaces. To model caustics, a photon map extension was implemented into the *Radiance* environment by Roland Schregle [13,14]. Photon mapping consists of two steps where light photons are initially emitted from a light source into a scene and then collected (gathered) in a secondary regular backward raytracing step.

The aim of our research is to evaluate the ability of the photon mapping approach to accurately predict light distributions caused by curved glass objects. Our validation consists of a series of comparative physical measurements and digital lighting simulations. Using 3D printed glass geometry as the benchmark for light-redirecting building components, our tests evaluate real-world physical artefacts of high geometric complexity. In order to accurately benchmark the digital simulations, digital-physical pairs of the experimental setups were used.

Current trends in architectural design require novel digital design tools that enable the engineering and fabrication of geometrically varied building components in high profile buildings. Curved building envelopes such as the King Abdullah Financial District Metro Station in Riyadh, designed by Zaha Hadid Architects (ZHA) with complex glazing systems and reflective metal façade elements, challenge existing lighting simulation frameworks (Figure 1). In order to fully leverage the new geometric freedom to construct spaces with superior environmental performance and occupant well-being, lighting simulation capabilities must also expand.

***Figure** 1: Geometrical complexity in a glazed building envelope, King Abdullah Financial District Metro Station in Riyadh, designed by Zaha Hadid Architects. Exterior rendering (left), construction of façade diagrid (middle, photograph by Faisal Bin Zarah) and close-up of detailed facade mockup (right) (all images property of RDA and courtesy of ZHA).*

Previously tested approaches for modeling and simulating light behavior in so-called complex fenestration systems (CFS) include the use of Bidirectional Scattering Distribution Functions (BSDF) that have been successfully modeled and implemented into the *Radiance* platform to accurately depict reflective window blinds[15], optical louver systems [9], prismatic window film [16] or the use of function files for laser cut panels (LCP) [17,18]. A BSDF is a four-dimensional mathematical function that describes the optical transmittance or reflectance of a material for all combinations of incoming and outgoing rays. BSDFs are determined via modeling or measurements in a goniophotometer [19]. As a further challenge, even if a goniophotometer is available, for some samples with pronounced specular or caustic components, it remains difficult to detect peaks within the distribution. In addition, goniophotometers accommodate limited sample sizes, assuming that the optical behavior of larger components is the same as that of the sample. *Radiance* function files allow users to define specific mathematical functions that describe the light-redirecting behavior of a material [20]. Furthermore, combining BSDF based lighting simulations with EnergyPlus models allows for the development of both daylight redirecting and energy harvesting systems [21].

For more complex building envelopes, where material parameters and geometry vary across a surface, BSDF and function file methods cannot be reliably applied. In order to represent and simulate the performance of parametric façades with highly differentiated geometries, photon mapping offers an alternative approach by considering the complete digital geometric representation of a system of any size.

Ongoing advances in additive manufacturing have led to the development of novel material systems that could be further developed for use as architectural components towards large-scale applications in the built environment. Out of their research around additive manufacturing of optically transparent glass, the Mediated Matter Group at the MIT Media Lab created a manufacturing platform for the fabrication of large-scale components (Figure 2).

Figure 2*: Additive manufacturing of optically transparent glass by the Mediated Matter Group, MIT Media Lab. Glass object with caustic pattern (top left), 3D printing process (top right), variety of printable objects (bottom left) and glass column with inserted light (bottom right) (all images courtesy of the Mediated Matter Group).*

Such an extrusion-based 3D printing technology enables the use of computer-aided design (CAD) models (Klein et al. 2015) to specify geometry and surface structure of glass components. Unlike the flat float glass that is traditionally used in buildings, 3D printed glass has an inherent depth and surface geometry that can be customized across every element. The optical clarity of glass creates highly complex caustic patterns when light is projected through a printed object. Curvature and surface texture, which consists of striations and bulges caused by the 3D printing process, offer a high degree of control over the reflection, redirection, and shading of light passing through the transparent objects (Inamura et al. 2018). It should be noted that even though the manufacturing process is digitally controlled, 3D printing of glass currently creates unforeseeable extrusion details on the millimeter scale that add to the aesthetic appeal and uniqueness of each sample but cannot be fully predicted in advance. In order to create reliable digital pairs of the test objects that were investigated in this study, the authors used post-processed 3D scans of the printed objects that emulated these extrusion details (see below). Physical scale models have been validated to accurately model light through CFS and predict daylight luminance values as well as daylight probabilities of interiors [22,23]. In the case of glass 3D printing, the properties of a component cannot be scaled down to maquette scale as they are inherent to the full-scale manufacturing process. Therefore, we created our digital, physical pairs in 1:1 scale.

When deployed in a real-world context, possible visual discomfort, glare, as well as light and shadow of a transparent object must be considered in its design. For this study, the authors therefore collected HDR photographs and photon map-based simulations of 3D printed objects under a variety of electrically lit and daylight conditions. In HDR images, each pixel has an RGB color value as well as an absolute luminance value. The authors then used the images to evaluate whether photon mapping can be used for simulating both a 3D printed object's overall architectural appearance as well as its impact on visual quality and comfort in the surrounding space.

2 Methodology

2.1 Validation Experiments

For the benchmarking exercise described above, three 3D printed glass objects were used: a standard cylindrical tube, a symmetrical three-bulge extrusion, and an irregular four-bulge extrusion (Table 1). As a result of the additive manufacturing process, the objects feature a rippled layering on their exterior surface with visible layers at 5 mm intervals. The interior of the objects consists of solid glass without defects or layering, enabling full optical transparency. The geometric complexity of the rippled layering, in combination with the freedom of form enabled through the manufacturing process, creates glass pieces with highly complex doubly curved lens geometries. This makes the prediction and simulation of light behavior passing through a component computationally expensive and inherently difficult.

Object Nr.	1	2	3
Description	Cylindrical Tube	Three Bulges	Four Bulges
Dimensions	217 x 217 x 209 mm	262 x 283 x 201 mm	231 x 245 x 201 mm
Polygon mesh face count	263783	244668	237827

Table 1: *Comparison of 3D printed glass objects used in validation experiments.*

The authors conducted two sets of experiments to validate the photon map:

- Experiment A: Digital-physical pair of glass objects under a single light electric light source
- Experiment B: Digital-physical pair of glass objects under variable daylight conditions

To capture the lit scenes and the physical quantity of luminance, as per the protocol presented by Inanici and Galvin, and Jones and Reinhart [10,24], a series of photographs were combined into an HDR image where the pixel brightness per image was matched with the measurements taken from a luminance meter. To record our physical experiments, a Canon EOS 5D Mark III full-frame digital camera outfitted with a 24-70 mm F2.8 Canon lens and a Konica Minolta LS-110 luminance meter were used.

2.2 Experimental Setup A – Interior Lighting

The first experimental setup consisted of a series of 3D printed glass objects (Table 1: Object Nr. 1, 2, 3) that were centred on an 80 x 80 cm grid for reference purposes (Figure 3). The digital camera is mounted vertically on an aluminium scaffold above the test objects to capture the caustic patterns with as little distortion as possible on the flat grid. A luminance meter is used to calibrate each photograph. Additionally, a reference image without a glass piece was taken to show the distribution of light without caustic reflections. In blacked out surroundings, a single light source was directed towards the glass pieces: A Soraa PAR 20 10.8 W spotlight was placed 22 cm above the ground plane, over the centre of the grid.

2.3 Experimental Setup B – Exterior Lighting

The daylighting conditions were tested in Cambridge, Massachusetts, USA on the roof of the MIT Media Lab (42°21'36.9"N, 71°05'14.9"W). To mimic an architectural interior space with a 3D printed glass envelope, an enclosure of 72 x 102 x 21 cm was constructed with an opening that fit the cylindrical glass tube (Table 1: Object Nr. 1). The dimensions of the box were determined by the size of the 3D printed glass sample piece. The height of the box corresponds to the height of the sample piece. This is in order to provide insight into how a facade with 3D printed glass components could look like from the interior of a building. The width and depth of the box were scaled so the primary caustic patterns would be visible on the ground and ceiling surface of the enclosure. All surfaces were made from the same white, coated foamboard. The glass tube was placed on the side of the space and blocked the only direct light into the space (Figure 4). On the back side of the box, a Canon EOS 5D Mark III full-frame camera with a 24-70mm F2.8 Canon lens was mounted on a tripod and placed at the secondary opening to record images of sunlight passing through the glass cylinder. Data was captured through HDR photographs every half hour from 08:00 to 16:00 on October 19, 2019. The sky was clear without cloud cover obstructing the sun. Continuous measurement of the luminance levels on a fixed point inside the box was conducted with the Konica Minolta LS-110 luminance meter.

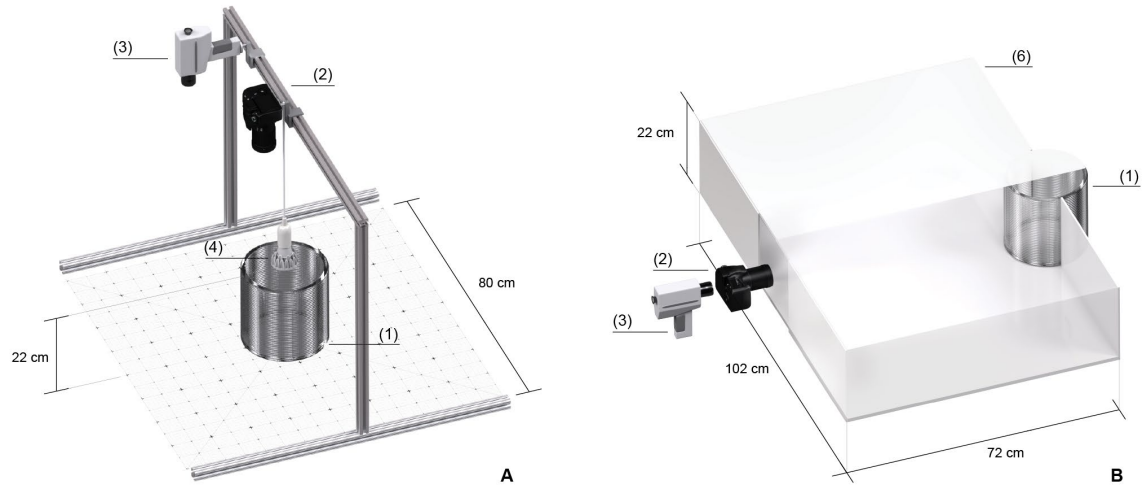

***Figure 3**: Schematics of experimental setups A and B with 3D printed glass object (1), digital camera (2) and luminance meter (3). Experiment A is set up in an indoor environment with the artificial light source, Soraa Par20 10.8W (4). Experiment B is conducted in a closed box (6) in an outdoor environment.*

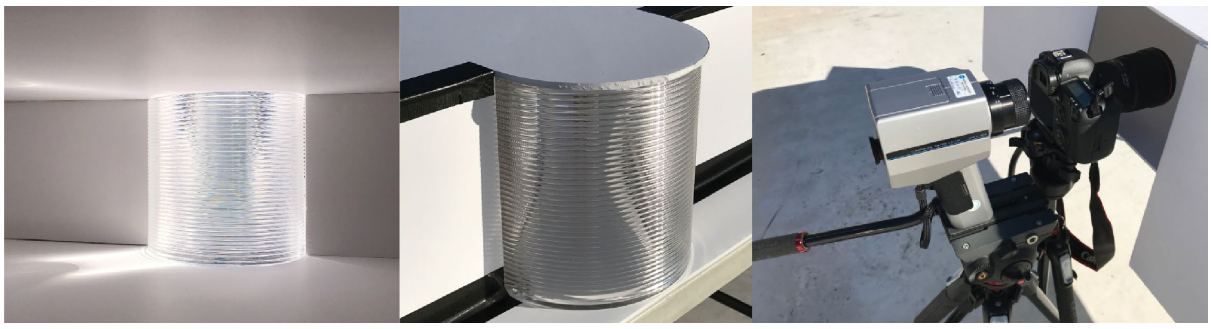

***Figure 4:** Photographs of physical setup of experiment B with interior view of lit cylinder (left). An exterior view of the 3D printed glass cylinder in sunlight (middle) and the measurement via digital camera, Canon EOS 5d Mark III and the Konica Minolta LS-110 luminance meter (right).*

2.4 Geometry Workflow

Although deposition of the glass in the manufacturing process has proven to be highly precise [25], the actual geometry of a 3D printed glass object exhibits artefacts that stem from temperature and viscosity fluctuation in the manufacturing process. To create a high-resolution mesh that accurately

represents the surface detail of a 3D printed glass piece, a digital post-process had to be developed, as shown in Figure 5. The workflow illustrates how a fine geometric detail was applied to a simulation geometry of a larger scale. In this case, a 3D printed glass sample part with a layer height of 5 mm in combination with an abstract input geometry was used to create a digital model of each physical object shown in Table 1.

Because of the dimensions of the 3D glass prints used in our physical experiments, a full 3D scan proved to be technically unfeasible with available equipment. Scanners or photogrammetry methods that are used for large scale objects fail to capture the detail of the 3D printed layers that are needed for an accurate digital simulation. A state of the art Artec Leo 3D scanner [26] was tested and did not provide the required surface details. As a result, we construct our workflow around 3D scanning of a sample piece, small enough to be able to be scanned with a laser scanner on a rotary bed. The sample piece with the dimensions 16 x 73 x 49 mm was a section cut from a larger 3D printed cylinder and the same print parameters as our test pieces, ensuring the same layer heights and thickness. As a first step (a), a NextEngine 2020i 3D laser scanner is used to capture the detail of a small 3D printed glass sample. For the laser to detect the surface of the sample, the glass is coated using a water soluble SKD-S2 Aerosol Developer Spray. The surface scan data is reconstructed as a mesh using ScanStudio HD [27]. The triangulated mesh we retrieve has inherent noise and artefacts, such as overlapping and non-manifold mesh faces, that make it impossible to be used directly for an accurate simulation. A postprocessing step of converting the triangulated mesh into a smooth and continuous surface is needed. We conduct this re-meshing (b) using the 3D modeling package Autodesk Maya [28], where the triangulated surface serves as a constraint for the generation of a quadrilateral mesh surface that approximates the noisy 3D scanned mesh of the sample part. For continuous regular layering as in our sample part the quadrilateral mesh surface can be converted into a cross section curve to smoothly represent both sides of the object as non-uniform rational basis spline (NURBS). A new input geometry is created in Rhinoceros 3D (Rhino, [29]) that represents the overall dimensions of the final geometry without any details (c). The input geometry has the exact dimensions of the glass test pieces (Table 1). Using or a regular quadrilateral mesh or NURBS curve representation of the surface geometry of the sample part, the geometric detail of our scan can be transferred and mapped onto the input geometry with standard modeling operations (d). This results in a high-resolution mesh, creating an accurate digital model that applies the geometric detail of the sample part to our input geometry.

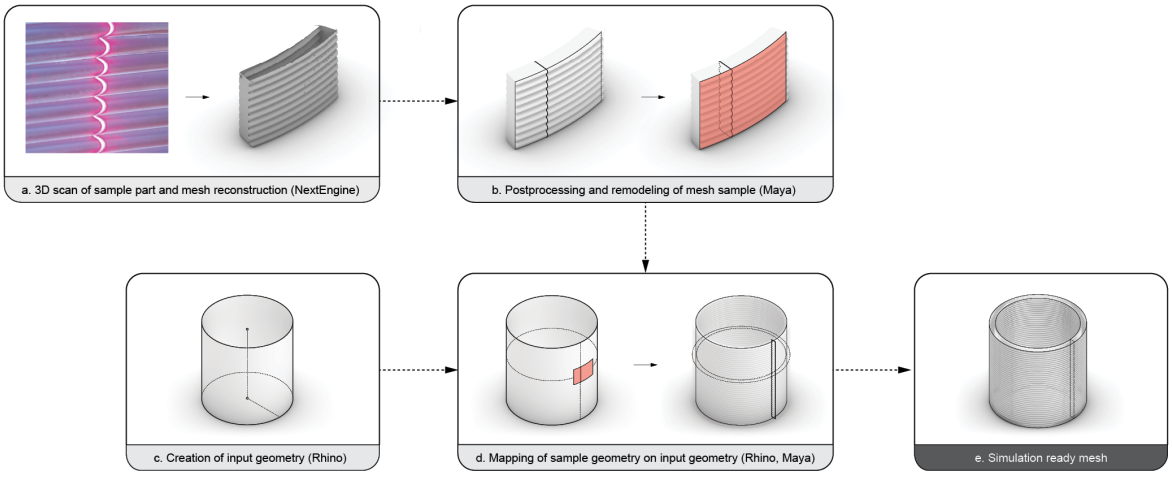

***Figure 5**: Remodeling workflow for 3D printed glass. A sample geometry is scanned and mapped onto a final geometry to create the mesh used in the lighting simulations (A-E).*

2.5 Digital Simulation

A digital scene of each physical setup as described in Figure 3 was created in Rhino and exported as an OBJ file. For an accurate representation of the 3D printed glass geometry, a high-resolution mesh

was produced of each glass piece using the described geometry workflow. The light simulations were produced with *Radiance* in photon mapping mode. The geometries and lights (sky and spotlight) were converted into the *Radiance* file format and assembled as a *Radiance* scene. For Experiment A, the spotlight used in the physical setup was represented using an IES file provided by the manufacturer. To test its accuracy, a calibration image using the light without any geometry was produced.

For Experiment B, the *Radiance* program *gendaylit* was used to create a sky according to the Perez sky model [30]. With measurement data provided by the MIT Weather Station, total horizontal solar radiation was first split into direct normal irradiance and diffuse-horizontal irradiance using the *gen_reindl* program in Daysim [31] and then input into *gendaylit*. Measured radiation on October 19, 2019, a sunny day with no cloud cover, ranged from 147 kWh/m^2 (08:00) to 601 kWh/m^2 (12:25).

The *Radiance* photon map extension, developed by Roland Schregle [14], was used to compute the caustic reflections of the glass objects. In a first assessment, caustic photon maps in various resolutions were produced to determine an optimal photon count, balancing render speed with ability to depict the required caustic details. Photon maps were computed on a Linux machine with following specifications: *128 Gb ddr4* Ram, *Nvidia RTX Geforce 2080* Graphics card, *3.0 Ghz AMD Threadripper 2990wx 32*-Core Processor.

A sample *Radiance* command setup involves 4 steps (Table 2), consisting of scene assembly (Step 1), photon map assembly (Step 2) image generation (Step 3) and image filtering (Step 4). The *Radiance* materials for the 3D printed glass for both experiments and for the interior walls of the box in experiment B are specified in Table 3.

Step 1	oconv	{skyfile}.rad {meshfile}.rad > {scenefile}.oct
Step 2	mkpmap	-n 32 -t 30 -apg {globalpmapfile}.gpm 50k -apc {causticmapfile}.cpm 50m {scenefile}.oct
Step 3	rpict	-vf {viewfile}.vf -af {ambtempfile}.amb -x 3200 -y 2400 -ps 8 -pt .15 -pj .6 -dj 0 -ds .5 -dt .5 -dc .25 -dr 0 -dp 128 -st .85 -ab 4 -aa .15 -ar 512 -ad 2048 -as 512 -lr 4 -lw .05 -ap {globalpmapfile}.gpm 100 2000 -ap {causticmapfile}.cpm 100 2000 {scenefile}.oct > {rpictimage}.hdr
Step 4	pfilt	pfilt -r .6 -x /4 -y /4 {rpictimage}.hdr > {outputimage}.hdr

Table 2: *Sample commands for the photon mapping approach (variable files indicated with {file})*

Glass	**White**
void dielectric print_glass	void plastic reflective_white_box
0	0
0	0
5 0.9 0.9 0.9 1.5 0	5 0.92 0.92 0.92 0.0135 0.0000

Table 3: *Radiance material definitions of the 3D printed glass material (Glass) and the box interior material (White)*

3 Results

The following sections describe the results of the physical validation experiments, including the HDR photographs of the 3D printed glass objects and the luminance measurements used to calibrate the photographs.

3.1 Results of Experiment A – Indoor Lighting

Results of Experiment A are depicted in Figure 7 and Figure 8. In Figure 7, side-by-side comparisons of false color HDR photographs (physical) and *Radiance* photon map renderings (digital simulation) show how accurately photon mapping predicted light behavior. The comparison cases show the physical setup without no object as photograph (p0) and simulation (s0). The three 3D printed glass objects from Table 1 are represented as both photograph of physical setup (p1, p2, p3) and digital *Radiance* simulation (s1, s2, s3). The black grid on the ground plane of the photographs was used to center the objects and maintain reference points for the calibration. The renderings feature a white

matte backdrop without a grid. Photon maps with 200 million caustic photons were rendered via the *Radiance -mkpmap* command. Both photographs and simulations have no post-production effects applied and were converted into false color for visual comparison purposes. They were remapped to a logarithmic (*log*) scale and a range of 1000 cd/m^2 with the *Radiance -fcolor* command. In all three cases, the overall lighting pattern on the grid below the glass objects look largely identical and include the same caustic hot spots.

Pairs of measured (physical) and simulated (digital) luminance levels across the center x-axis of the images for the same four cases are shown in Figure 8. In the photographs, the black gridlines of the calibration grid cause noise in the measured brightness plots. Noise in the *Radiance* from the photon map rendering results in slight distortions in the simulated brightness plots. Brightness values were obtained using the *Radiance* image analysis tool *-pcomp.* They are shown in a logarithmic scale for both measured and simulation. For more accurate comparisons, the curves were scaled and centered to adjust for slight deviations in the digital representation and to more accurately map the features of the physical tests. In order to minimize offsets from the noise from both gridlines and simulation, the data was filtered using an average smoothing and capped at a maximum of 1000 cd/m^2. The resulting curves were processed and have a root mean square of 16.7 % (test 0), 18.12 % (test 1), 7.97 % (test 2), 12.91 % (test 3). The resulting luminance sections exhibit largely similar behavior, except that the measured peaks tend to be somewhat more pronounced than in the simulations, whereas grain from the noise in the photon map distorts the results of the simulation slightly.

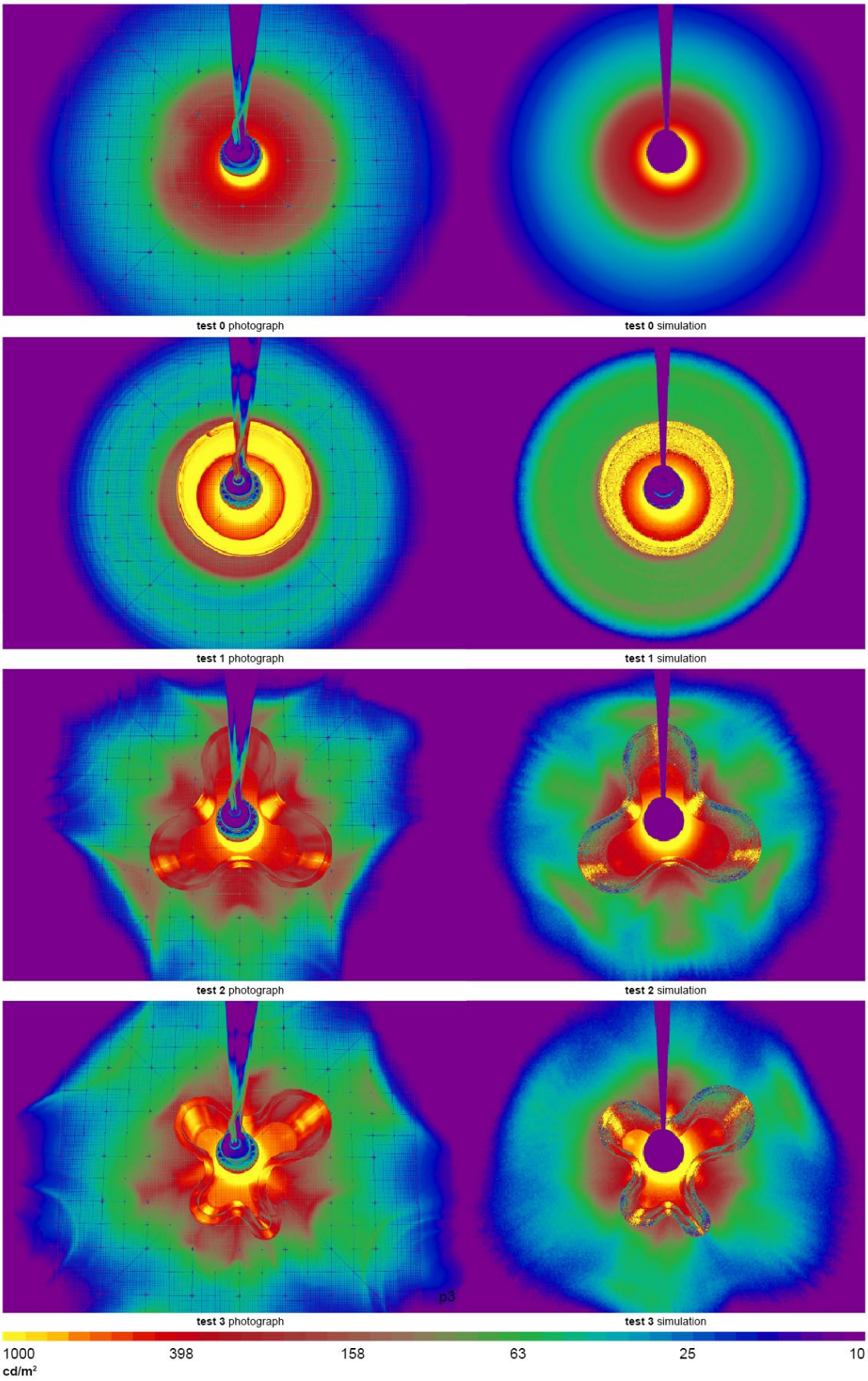

***Figure 6**: Comparison of HDR photograph and Radiance photon map simulation of no object (test 0), cylindrical tube (test 1), three bulges (test 2) and four bulges (test 3).*

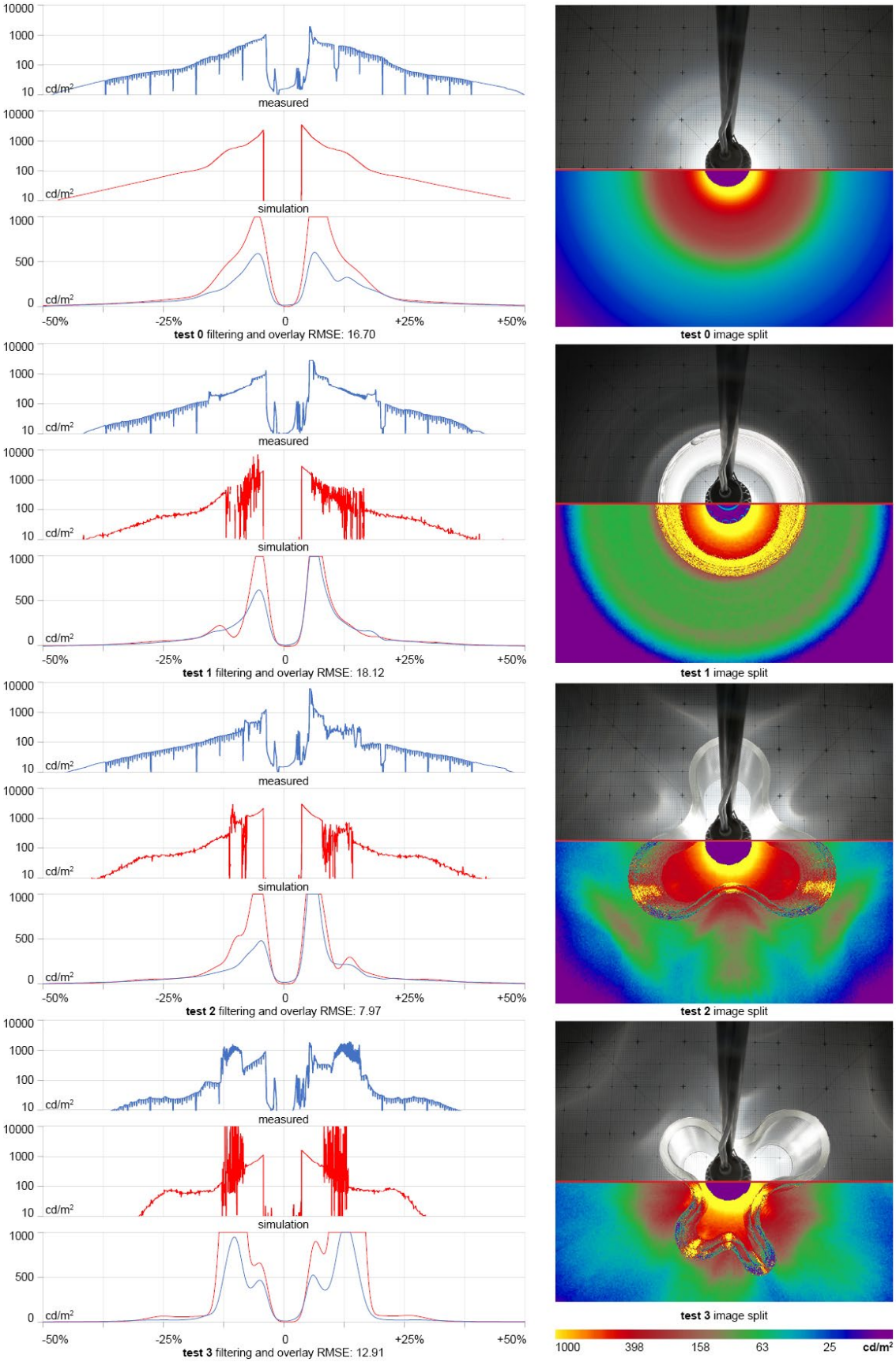

Figure 7: *Plots of brightness values (left) with measured and simulated luminance in logarithmic scale and a smoothened, scaled and capped overlay of both datasets in linear scale with the resulting root mean square error. Image split (right) shows an HDR photograph overlaid on the digital simulation with a red line indicating the position of the luminance measurements in the plots.*

3.2 Results of Experiment B – Exterior Lighting

Results of Experiment B are depicted in Figure 8. Qualitative comparisons show how the complex simulated (digital) caustic reflections exhibit the same patterns as their measured (physical) counterparts. Side-by-side comparisons of false color renderings and HDR photographs depict how higher concentrations of light at the top and bottom of the glass cylinder are always visible in both photograph and rendering. A key difference between photographs and renderings is the appearance of the glass itself as a source of glare. In the *Radiance* photon mapping simulation, the glass appears dark and only passes light into the interior. In a high resolution simulation, there appears to be significant noise in the areas with glass material in the simulation where some pixels would attribute to the glare. When scaling down the image, this information is not retained.

It should be noted that additional light-reflective structures in the physical environment were not simulated digitally. Although the experiment was fully exposed to sunlight and not shaded at any part of the day, additional secondary bounces of light through the camera hole and through the glass from additional surrounding objects were not considered. Furthermore, the simulation only considered a fixed set of ambient bounces that lit the space, so lighting levels may differ.

Figure 9 shows a comparative graph of luminance measurements of the *Radiance* simulation. The physical measurements with the luminance meter differed up to +/- 15% each time they were taken. Averages of three measurements taken at the same point at the same time are shown as data points of the measurements. To match the digital and physical measurements as closely as possible, an aerial average of a patch of approximately 25 cm^2 around the physical measurement point was averaged to obtain the digital simulation light luminance value from the calibrated *Radiance* image. The graph shows that the light levels in the interior of the box were predicted highly accurate. Furthermore, visual glare with a threshold of > 2000 Cd/m^2 was predicted successfully for all times of the day.

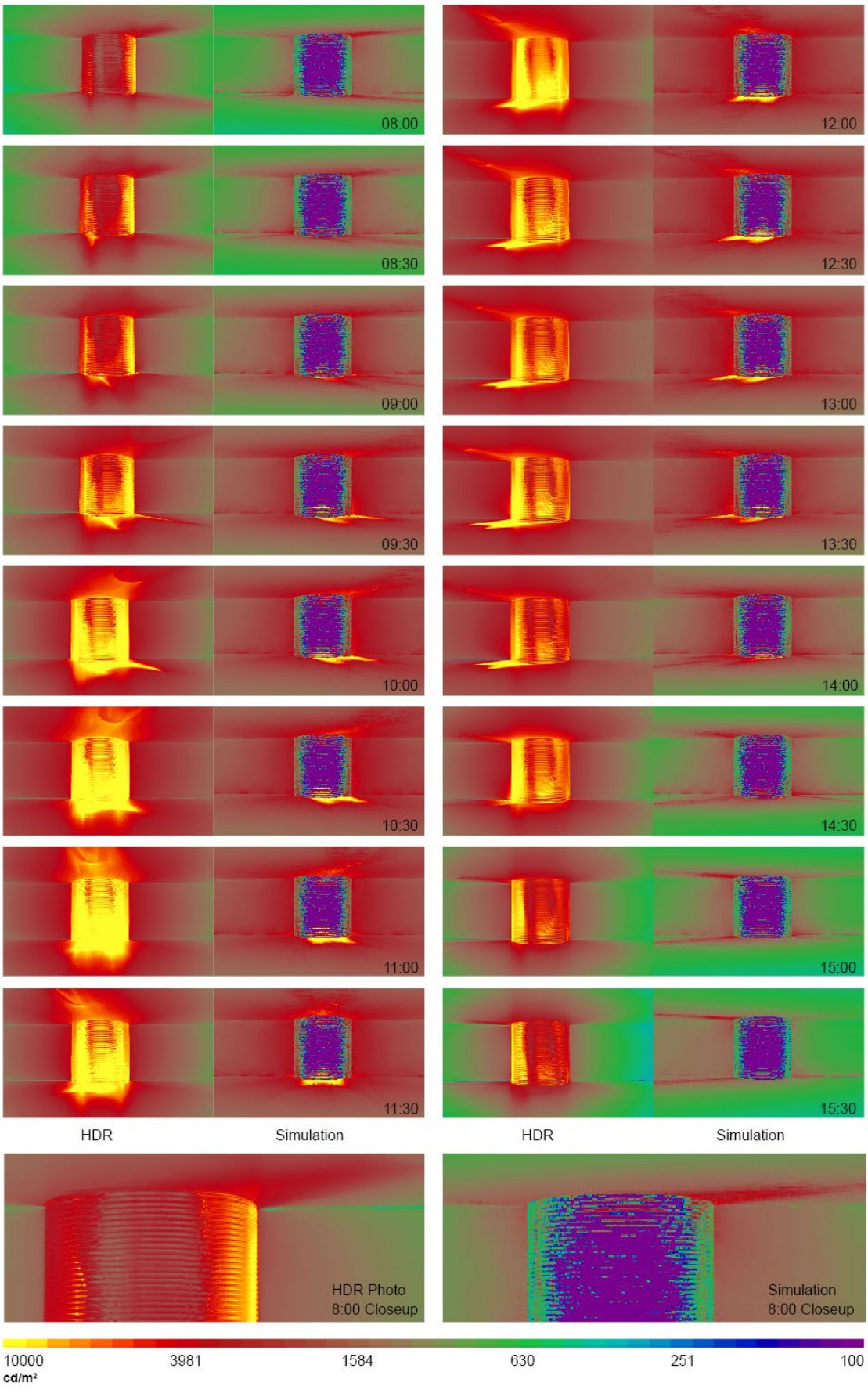

Figure 8: *3D printed glass cylindrical tube in daylight captured as false color HDR photographs and Radiance photon mapping simulations.*

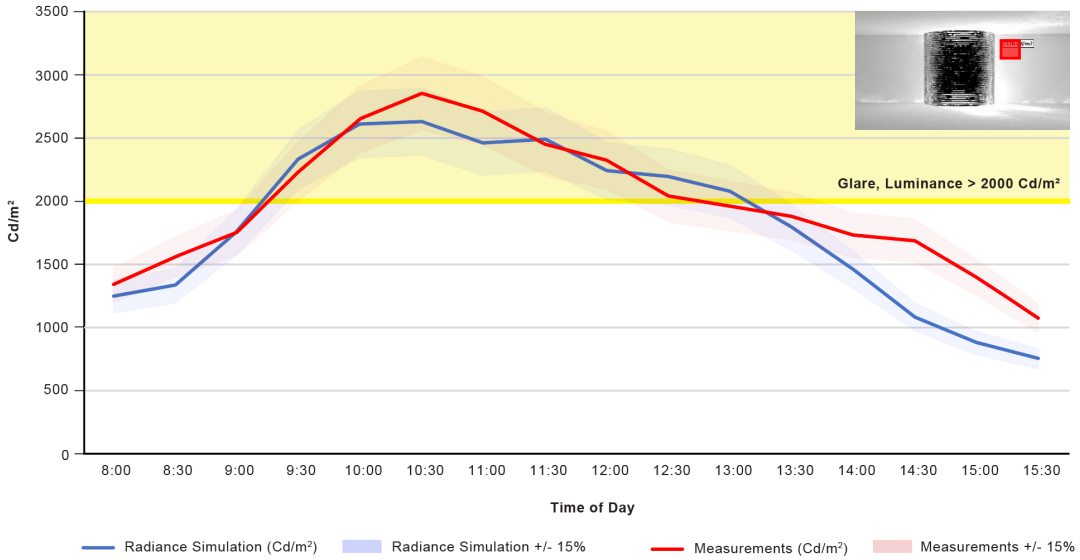

Figure 9: *Light level comparison, Cd/m², of a fixed point inside the box in Experiment B of both digital Radiance simulation and physical measurements. A sample image of the digital Radiance simulation at 9:30 am is depicted (top right corner). The red square indicates the area of where the luminance value average was measured. A visual glare threshold of > 2000 Cd/m² is displayed in yellow.*

4 Discussion

4.1 Discussion

The results indicated that the photon mapping approach is able to reliably simulate certain aspects of light distributions through complex 3D printed glass objects. Most notably, the method excels at predicting lighting patterns resulting from such objects as artistic luminaires or daylighting façade elements. It unfortunately is subject to the same limitation of other raytracing methods in that they generally fail to model scattering at the glass surface or within the glass due to material imperfections. Such scattering phenomena may lead to extremely high luminances, which are equally prone to trigger delight and glare. The authors attempted unsuccessfully to model the light scattering in *Radiance* by testing a series of material modifiers with varying roughness and indexes of refraction. Similar limitations were previously reported by Greenup, Edmonds, and Compagnon when they tried to simulate scattered lighting artefacts from laser cut panels [17]. Real-world fine-grained material imperfections inside materials can have large effects on light scattering and thus glare, making the latter extremely difficult to simulate.

In our Experiment B, light distribution in the daylit space itself created so much glare along the surrounding walls that traditional glare modeling methods predicted visual discomfort would occur at the same time for measurements and simulations (Figure 10). However, because the daylighting element itself was not detected as a glare source, one can easily imagine situations – e.g. in the presence of dark walls – in which the room does not contribute to glare. In this case, glare and visual discomfort would remain undetected by the photon map.

What do these results mean for designers? The authors recommend using the *Radiance* photon mapping approach for aesthetic explorations. Visual comfort studies should further pair digital models with physical explorations of parts of a façade or building. The following sections present additional modeling advice for setting up lighting simulations for complex 3D printed glass objects.

4.2 Geometric Detail

Successful simulation of complex geometries using *Radiance* photon mapping requires a highly accurate digital model. Capturing or modeling all relevant detail can require a significant effort. In the case of additive manufacturing, an abstracted design model is therefore not sufficient for simulation, even when it might be used in manufacturing of the object. Rather, the model must represent the physical outcome of the manufacturing process, including all significant geometric details. As shown in the presented research, a process like 3D printing glass must consider significant uncertainty due to material layering and composition. The 3D scanning and remodeling workflow in Figure 6 lends itself to the digital representation of such highly complex geometries. The geometric freedom enabled by additive manufacturing further increases the strain on a simulation engine. 3D scanning and accurate modeling are key steps in accurate high-resolution representation of complex geometries and their successful simulation.

Since the *Radiance* render engine relies on mesh geometries, it is important to consider the conversion process when working with NURBS geometry (for example by utilizing the Diva components inside of Rhino). An automatic conversion (e.g. by using an uncontrolled meshing operation) can lead to highly inaccurate results as shown in Figure 11, where two mesh geometries are compared. Automatic triangulation of a low-resolution mesh (a) did not suffice to accurately depict the caustic reflections. A manual adjustment and lowering of the maximum edge lengths in the meshing process created a mesh with higher resolution, successfully predicting continuous caustic patterns.

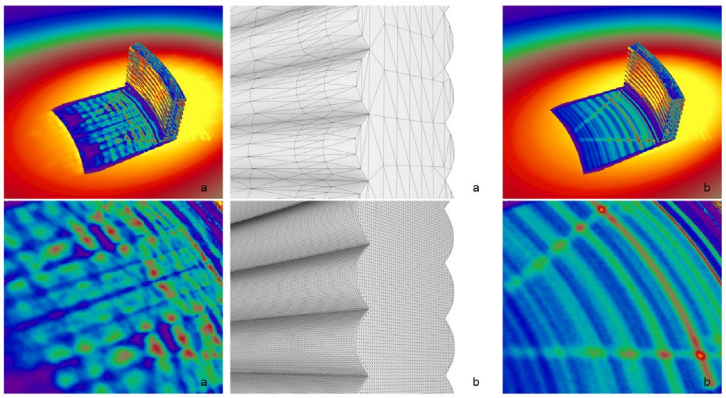

Figure 10: *Sources of error through low resolution mesh representation for the number of photons scattered in the scene. A low-resolution mesh (a) with 4915 faces is compared with a high-resolution mesh (b) with 370252 faces.*

4.3 Simulation Parameter Settings

As in the case of classic light-backward raytracing with *Radiance*, simulation parameters need to be set in accordance with the complexity of the problem at hand. For photon mapping, an adequate photon count must be chosen to be able to fully depict caustic details. For novel geometric structures, photon count must be determined iteratively and is difficult to predict, as a rule of thumb. It is dependent on the level of detail of the geometry and the lighting situation. For example, a comparative rendering in Figure 11 shows how photon count visibly increases in direct relation to the accuracy and resolution of the caustic map. We experienced a variety of simulation times depending on the photon count and the mesh resolution, ranging from five minutes to two hours. In the generation of the photon maps we made use of the multiprocessor capabilities implemented in the "-mkpmap -n" function, which makes it possible to run the photon mapping on 32 cores simultaneously.

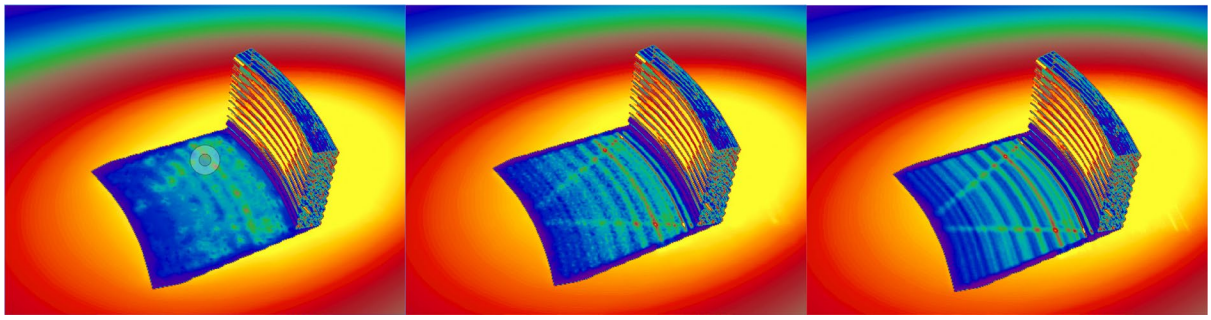

Figure 11: *Photon maps (left to right) with 10000 photons, 200000 photons and 10000000 photons increase the resolution and accuracy of the caustic simulation.*

4.3 Opportunities for Design

Reverse modeling of caustic lighting effects could enable future architectural components that can be shaped by real-world lighting properties while accounting for material imperfections. Our 3D scanning and modeling workflow can scale to fit a wide range of geometric features or geometrically complex building components and to various transparent materials. It enables daylight-conscious design and performative validation of novel architectural façade solutions or solar reflectors. It creates new opportunities for modeling irregular Fresnel lenses and curved mirror systems for light redirection and energy generation, including artistic exploration of glass technologies at the building and urban scales. Creating accurate virtual models of caustic reflections is a fundamental step in the production of 3D printed glass and other physical artefacts.

5 Conclusion

Daylight is a key factor in designing low-energy buildings and façades conscious of the environment and its inhabitants. Digital fabrication and additive manufacturing increase the parametric variability and adjustability of building components without further cost, and the full potential of these technologies cannot be realized without digital workflows that are able to leverage this geometric freedom into more performative building solutions.

Our research suggests that the *Radiance* toolset with the photon mapping approach to simulation provides the designer a clear idea of caustic patterns and light levels of interior spaces in highly complex glass systems. While we were able to predict when glare would occur within the space with some level of confidence, it should be noted that our simulations systematically underestimated brightness levels from the glass objects. One possible explanation is that raytracing generally, and photon mapping specifically, are not able to model light scattering due to material imperfections both at the surface and the interior of glass structures. Such material imperfections may result in objects where the glass structure itself can act as the glare source. By using digital and physical models complementary, ideally on a 1:1 scale, designers can study these effects in isolation before implementing their innovative lighting and daylighting systems in an entire building.

6 Acknowledgments

This research was primarily sponsored by The Mediated Matter research group at the MIT Media Lab. The 3D printed glass objects used in the experiments were created for the Lexus YET show by the Mediated Matter Group in collaboration with Lexus at the Milan Design Week, 2017. The authors would like to thank Michael Stern for his input on the Glass 3D printing process, Peter Houk for his introduction to glassmaking, Dr. Roland Schregle and Dr. Lars Grobe for their valuable help and initial discussions around photon mapping and Dan Weissman for his advice on the artificial lighting experiments.

7 References

[1] M. Woodward, Commercial Buildings Energy Consumption Survey (CBECS) Trends in Lighting in Commercial Buildings, (2017) 1–19. https://www.eia.gov/consumption/commercial/reports/2012/lighting/ (accessed March 10, 2019).

[2] E. Saratsis, T. Dogan, C.F. Reinhart, Simulation-based daylighting analysis procedure for developing urban zoning rules, Build. Res. Inf. 45 (2017) 478–491. https://doi.org/10.1080/09613218.2016.1159850.

[3] C.E. Ochoa, M.B.C. Aries, J.L.M. Hensen, State of the art in lighting simulation for building science: A literature review, J. Build. Perform. Simul. 5 (2012) 209–233. https://doi.org/10.1080/19401493.2011.558211.

[4] R. Ward, G. and Shakespeare, Rendering with Radiance: The Art and Science of Lighting Visualization, 1998.

[5] A. Galasiu, C.F. Reinhart, Current Daylighting Design Practice: A Survey, Build. Res. Inf. 36 (2007) 159–174.

[6] J. Mardaljevic, Validation of a Lighting Simulation Program under Real Sky Conditions, Light. Res. Technol. 27 (1995) 181–188.

[7] C.F. Reinhart, O. Walkenhorst, Dynamic RADIANCE-based Daylight Simulations for a full-scale Test Office with outer Venetian Blinds, Energy Build. 33 (2001) 683–697.

[8] C.F. Reinhart, M. Andersen, Development and validation of a Radiance model for a translucent panel, Energy Build. 38 (2006) 890–904.

[9] A. McNeil, E.S. Lee, A validation of the Radiance three-phase simulation method for modelling annual daylight performance of optically complex fenestration systems, J. Build. Perform. Simul. 6 (2012) 24–37. https://doi.org/10.1080/19401493.2012.671852.

[10] N.L. Jones, C.F. Reinhart, Experimental validation of ray tracing as a means of image-based visual discomfort prediction, Build. Environ. 113 (2017) 131–150. https://doi.org/10.1016/j.buildenv.2016.08.023.

[11] J.A. Jakubiec, C.F. Reinhart, DIVA 2.0: Integrating daylight and thermal simulations using rhinoceros 3D, DAYSIM and EnergyPlus, Proc. Build. Simul. 2011 12th Conf. Int. Build. Perform. Simul. Assoc. (2011) 2202–2209.

[12] R.M. Sadeghipour, M. Pak, Ladybug: a parametric environmental plugin for grasshopper to help designers create an environmentally-conscious design, in: Proc. BS2013 13th Conf. Int. Build. Perform. Simul. Assoc., Chambery, 2013. https://www.ibpsa.org/proceedings/bs2013/p_2499.pdf.

[13] R. Schregle, Bias Compensation for Photon Maps, Comput. Graph. Forum. 22 (2003) 729–742. https://doi.org/10.1111/j.1467-8659.2003.00720.x.

[14] R. Schregle, Daylight simulation with photon maps, Saarland University, 2004.

[15] K. Konis, E.S. Lee, Measured daylighting potential of a static optical louver system under real sun and sky conditions, Build. Environ. 92 (2015) 347–359. https://doi.org/10.1016/j.buildenv.2015.04.024.

[16] A. McNeil, E.S. Lee, J.C. Jonsson, Daylight performance of a microstructured prismatic window film in deep open plan offices, Build. Environ. 113 (2017) 280–297. https://doi.org/10.1016/j.buildenv.2016.07.019.

[17] P. Greenup, I. Edmonds, R. Compagnon, RADIANCE algorithm to simulate laser-cut panel

light-redirecting elements, Light. Res. Technol. - Light. RES TECHNOL. 32 (2000) 49–54. https://doi.org/10.1177/096032710003200201.

[18] L.O. Grobe, Photon mapping in image-based visual comfort assessments with BSDF models of high resolution, J. Build. Perform. Simul. 0 (2019) 1–14. https://doi.org/10.1080/19401493.2019.1653994.

[19] M. Andersen, J. deBoer, Goniophotometry and assessment of bidirectional photometric properties of complex fenestration systems , Energy Build. 38 (2006) 836–848.

[20] The RADIANCE 5.1 Synthetic Imaging System, (n.d.). https://floyd.lbl.gov/radiance/refer/ray.html (accessed March 5, 2020).

[21] A. Vlachokostas, N. Madamopoulos, Daylight and thermal harvesting performance evaluation of a liquid filled prismatic façade using the Radiance five-phase method and EnergyPlus, Build. Environ. 126 (2017) 396–409. https://doi.org/10.1016/j.buildenv.2017.10.017.

[22] A. Thanachareonkit, J.L. Scartezzini, Modelling Complex Fenestration Systems using physical and virtual models, Sol. Energy. 84 (2010) 563–586. https://doi.org/10.1016/j.solener.2009.09.009.

[23] M. Bodart, C. Cauwerts, Assessing daylight luminance values and daylight glare probability in scale models, Build. Environ. 113 (2017) 210–219. https://doi.org/10.1016/j.buildenv.2016.08.033.

[24] M. Inanici, J. Galvin, Evaluation of High Dynamic Range Photography as a Luminance Mapping Technique, Berkeley, CA, 2004. https://doi.org/10.2172/841925.

[25] J. Klein, M. Stern, G. Franchin, M. Kayser, C. Inamura, S. Dave, J.C. Weaver, P. Houk, P. Colombo, M. Yang, N. Oxman, Additive Manufacturing of Optically Transparent Glass, 3D Print. Addit. Manuf. 2 (2015) 92–105. https://doi.org/10.1089/3dp.2015.0021.

[26] Artec3d, Artec Leo 3D Scanner, (2020). https://www.artec3d.com/portable-3d-scanners/artec-leo (accessed May 5, 2020).

[27] NextEngine, ScanStudioHD, (2020). http://www.nextengine.com/products/scanstudio-hd/ (accessed May 5, 2020).

[28] Autodesk, Maya, (2020). https://autodesk.com/maya (accessed May 5, 2020).

[29] R. McNeel & Associates, Rhinoceros3d, (2020). https://www.rhino3d.com.

[30] R. Perez, R. Seals, J. Michalsky, All-weather model for sky lumina nce distribution - preliminary configuration and validation, Sol. Energy. 50 (1993) 235–245.

[31] D.T. Reindl, W.A. Beckman, J.A. Duffle, Diffuse fraction correlations, (1990).